

Task-dependent control of open quantum systems

Jens Clausen,^{1,2} Guy Bensky,³ and Gershon Kurizki³

¹*Institute for Quantum Optics and Quantum Information,
Austrian Academy of Sciences, Technikerstr. 21a, A-6020 Innsbruck*

²*Institute for Theoretical Physics, University of Innsbruck, Technikerstr. 25, A-6020 Innsbruck, Austria*

³*Department of Chemical Physics, Weizmann Institute of Science, Rehovot, 76100, Israel*

(Dated: June 15, 2018)

We develop a general optimization strategy for performing a chosen unitary or non-unitary task on an open quantum system. The goal is to design a controlled time-dependent system Hamiltonian by variationally minimizing or maximizing a chosen function of the system state, which quantifies the task success (score), such as fidelity, purity, or entanglement. If the time-dependence of the system Hamiltonian is fast enough to be comparable or shorter than the response-time of the bath, then the resulting non-Markovian dynamics is shown to optimize the chosen task score to second order in the coupling to the bath. This strategy can protect a desired unitary system evolution from bath-induced decoherence, but can also take advantage of the system-bath coupling so as to realize a desired non-unitary effect on the system.

PACS numbers: 03.65.Yz, 03.67.Pp, 37.10.-x, 02.60.-x

Keywords: decoherence, open systems, quantum information, decoherence protection, quantum error correction, computational techniques, simulations

I. INTRODUCTION

Due to the ongoing trends of device miniaturization, increasing demands on speed and security of data processing, along with requirements on measurement precision in fundamental research, quantum phenomena are expected to play an increasing role in future technologies. Special attention must hence be paid to omnipresent decoherence effects. These may have different physical origins, such as coupling of the system to an external environment (bath) [1] or to internal degrees of freedom of a structured particle [2], noise in the classical fields controlling the system, or population leakage out of a relevant system subspace [3]. Formally, their consequence is always a deviation of the quantum state evolution (error) with respect to the expected unitary evolution if these effects are absent [4]. In operational tasks such as the preparation, transformation, transmission, and detection of quantum states, these environmental couplings effects are detrimental and must be suppressed by strategies known as dynamical decoupling [5–8], or the more general dynamical control by modulation [9–13].

There are however tasks which cannot be implemented by unitary evolution, in particular those involving a change of the system’s state entropy [14, 15]. Such tasks necessitate a coupling to a bath and their efficient implementation hence requires *enhancement* of this coupling. Examples are the use of measurements to cool (purify) a system [16–19] or manipulate its state [20–22] or harvest and convert energy from the environment [23–27].

A general task may also require state and energy transfer [28], or entanglement [29] of non-interacting parties via *shared* modes of the bath [30, 31] which call for maximizing the shared (two-partite) couplings with the bath, but suppressing the single-partite couplings.

It is therefore desirable to have a general framework

for optimizing the way a system interacts with its environment to achieve a desired task. This optimization consists in adjusting a given “score” that quantifies the success of the task, such as the targeted fidelity, purity, entropy, entanglement, or energy by dynamical modification of the system-bath coupling spectrum on demand. The goal of this work is to develop such a framework.

The remainder of the paper is organized as follows. In Sec. II we state the problem formally and provide general expressions for the change of the score over a fixed time interval as operator and matrix spectral overlap. In Sec. III we discuss a general solution in terms of an Euler-Lagrange optimization. In Sec. IV we apply the approach to the protection of a general quantum gate, which requires minimizing any coupling to the bath, whereas in Sec. V we consider the complementary case of *enhancing* the system-bath coupling in order to modify the purity (entropy) of a qubit. Open problems are outlined and an outlook is presented in Sec. VI. Supplementary information is provided in Apps. A and B.

II. OVERLAP-INTEGRAL FORMALISM

A. Fixed time approach

Assume that a quantity of interest (“score”) can be written as a real-valued function $P(t) = P[\hat{\rho}(t)]$ of the system state $\hat{\rho}(t)$ at a given time t . This might be, for example, a measure of performance of some input-output device that is supposed to operate within a predefined cycle/gate time t . Depending on the physical problem and model chosen, extensions and generalizations are conceivable, such as a comparison of the outcome for different t (on a time scale set by a constraint) [28], a time average $P = \int d\tau f(\tau)P[\hat{\rho}(\tau)]$ with some probability density

$f(\tau)$ [32], or a maximum $P(t) = \max_{\tau \in [0, t]} P[\hat{\rho}(\tau)]$ [33]. Here we restrict ourselves to the “fixed-time” definition as given above. Our goal is to generate, by means of classical control fields applied to the system, a time dependence of the system Hamiltonian within the interval $0 \leq \tau \leq t$ that adjusts $P(t)$ to a desired value. In particular, this can be an optimum (i.e. maximum or minimum) of the possible values of P . Assume that the initial system state $\hat{\rho}(0)$ is given. The *change* to the “score” over time t , is then given by the first-order Taylor expansion in a chosen basis

$$P(t) \approx \sum_{mn} \frac{\partial P}{\partial \rho_{mn}} \Delta \rho_{mn} = \text{Tr}(\hat{P} \Delta \hat{\rho}), \quad (1)$$

where the expansion coefficients

$$\left(\frac{\partial P}{\partial \rho_{mn}} \right)_{t=0} \equiv (\hat{P})_{nm} \quad (2)$$

are the matrix elements (in the chosen basis) of a Hermitian operator \hat{P} , which is the gradient of $P[\hat{\rho}(t)]$ with respect to $\hat{\rho}$ at $t=0$, i.e., we may formally write $\hat{P} = (\nabla_{\hat{\rho}} P)_{t=0}^T = (\partial P / \partial \hat{\rho})_{t=0}^T$. In what follows, it is \hat{P} which contains all information on the score variable. Note that the transposition applied in Eq. (2) simply allows to express the sum over the Hadamard (i.e. entrywise) matrix product in Eq. (1) as a trace of the respective operator product $\hat{P} \Delta \hat{\rho}$.

Let us illustrate this in two examples. If P is the expectation value of an observable (i.e. Hermitian operator) \hat{Q} , so that $P = \text{Tr}(\hat{\rho} \hat{Q})$, then Eq. (2) just reduces to this observable, $\hat{P} = \hat{Q}$. If P is the state purity, $P = \text{Tr}(\hat{\rho}^2)$, then Eq. (2) becomes proportional to the state, $\hat{P} = 2\hat{\rho}(0)$. Note that the score P is supposed to reflect the environment (bath) effects and not the internal system dynamics.

Equation (1) implies that $\Delta \hat{\rho}$ and with it P are small. Hence $\Delta \hat{\rho}$ must refer to the interaction picture and a weak interaction, while $P[\hat{\rho}(t)]$ should not be affected by the internal dynamics [so that no separate time dependence emerges in Eq. (1), which is not included in the chain-rule derivative]. In the examples above, this is obvious for state purity, whereas an observable \hat{Q} might be thought of co-evolving with the internal dynamics.

Our starting point for what follows is simply the relation $P = \text{Tr}(\hat{P} \Delta \hat{\rho})$ with some Hermitian \hat{P} , whose origin is not relevant.

B. Role of averaged interaction energy

Equation (1) expresses the score P as an overlap between the gradient \hat{P} and the change of system state $\Delta \hat{\rho}$. In order to find expressions for P in terms of physically insightful quantities, we decompose the total Hamiltonian into system, bath, and interaction parts,

$$\hat{H}(t) = \hat{H}_S(t) + \hat{H}_B + \hat{H}_I, \quad (3)$$

and consider the von Neumann equation of the total (system and environment) state in the interaction picture,

$$\frac{\partial}{\partial t} \hat{\rho}_{\text{tot}}(t) = -i[\hat{H}_I(t), \hat{\rho}_{\text{tot}}(t)], \quad (4)$$

$[\hat{H}_I(t) = \hat{U}_F^\dagger(t) \hat{H}_I^{(S)}(t) \hat{U}_F(t)$, (S) denoting the Schrödinger picture and $\hat{U}_F(t) = \text{T}_+ e^{-i \int_0^t d\tau [\hat{H}_S(\tau) + \hat{H}_B]}$]. Its solution can be written as Dyson (state) expansion

$$\begin{aligned} \hat{\rho}_{\text{tot}}(t) &= \hat{\rho}_{\text{tot}}(0) + (-i) \int_0^t dt_1 [\hat{H}_I(t_1), \hat{\rho}_{\text{tot}}(0)] \\ &+ (-i)^2 \int_0^t dt_1 \int_0^{t_1} dt_2 [\hat{H}_I(t_1), [\hat{H}_I(t_2), \hat{\rho}_{\text{tot}}(0)]] + \dots, \end{aligned} \quad (5)$$

which can be obtained either by an iterated integration of (4) or from its formal solution

$$\hat{\rho}_{\text{tot}}(t) = \hat{U}_I(t) \hat{\rho}_{\text{tot}}(0) \hat{U}_I^\dagger(t), \quad \hat{U}_I(t) = \text{T}_+ e^{-i \int_0^t dt' \hat{H}_I(t')}, \quad (6)$$

by applying the Magnus (operator) expansion

$$\begin{aligned} \hat{U}_I(t) &= e^{-it \hat{H}_{\text{eff}}(t)}, \quad (7) \\ \hat{H}_{\text{eff}}(t) &= \frac{1}{t} \int_0^t dt_1 \hat{H}_I(t_1) \\ &- \frac{i}{2t} \int_0^t dt_1 \int_0^{t_1} dt_2 [\hat{H}_I(t_1), \hat{H}_I(t_2)] + \dots, \end{aligned} \quad (8)$$

expanding in (6) the exponential $\hat{U}_I = \hat{U}_I(\hat{H}_{\text{eff}})$ and sorting the terms according to their order in \hat{H}_I .

We assume that initially, the system is brought in contact with its environment (rather than being in equilibrium with it), which corresponds to factorizing initial conditions $\hat{\rho}_{\text{tot}}(0) = \hat{\rho}(0) \otimes \hat{\rho}_B$. The environment is in a steady state $[\hat{\rho}_B, \hat{H}_B] = 0$, so it is more adequate to speak of a “bath”. Tracing over the bath in Eq. (5) then gives the change of system state $\Delta \hat{\rho} = \hat{\rho}(t) - \hat{\rho}(0)$ over time t , which we must insert into Eq. (1). We further assume a vanishing bath expectation value of the interaction Hamiltonian,

$$\langle \hat{H}_I \rangle_B \equiv \text{Tr}_B(\hat{\rho}_B \hat{H}_I) = \hat{0}. \quad (9)$$

As a consequence, the “drift” term corresponding to the first order in Eq. (5) vanishes, and we only consider the second order term as the lowest non-vanishing order approximation. Finally, we assume that the initial system state commutes with \hat{P} ,

$$[\hat{\rho}(0), \hat{P}] = 0. \quad (10)$$

In the language of control theory, $\text{Tr}[\hat{\rho}(0) \hat{P}]$ is a “kinematic critical point” [34] if Eq. (10) holds, since $\text{Tr}[e^{i\hat{H}} \hat{\rho}(0) e^{-i\hat{H}} \hat{P}] = \text{Tr}[\hat{\rho}(0) \hat{P}] + i \text{Tr}(\hat{H} [\hat{\rho}(0), \hat{P}]) + \mathcal{O}(\hat{H}^2)$ for a small arbitrary system Hamiltonian \hat{H} . Since we consider $\hat{\rho}$ in the interaction picture, Eq. (10) means that the score is insensitive (in first order) to a bath-induced

unitary evolution (i.e., a generalized Lamb shift) [30]. The purpose of this assumption is only to simplify the expressions, but it is not essential. Physically, one may think of a fast auxiliary unitary transformation that is applied initially in order to diagonalize the initial state in the eigenbasis of \hat{P} . Modifications to be made if Eq. (10) does not hold are provided in App. B.

To lowest (i.e., second) order we then evaluate Eq. (1) for the score change as

$$P = t^2 \langle [\hat{H}, \hat{P}] \hat{H} \rangle, \quad \hat{H} = \frac{1}{t} \int_0^t d\tau \hat{H}_I(\tau), \quad (11)$$

where $\langle \cdot \rangle = \text{Tr}[\hat{\rho}_{\text{tot}}(0)(\cdot)]$. This expresses the change of score in terms of the interaction Hamiltonian, averaged in the interaction picture over the time interval of interest. Our scheme is summarized in Fig. 1.

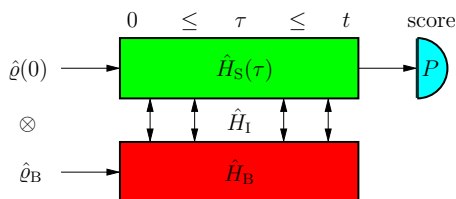


FIG. 1: Our control scheme: a system is brought in contact with a bath over a fixed time interval $0 \leq \tau \leq t$ during which the time dependence of the system Hamiltonian $\hat{H}_S(\tau)$ is chosen such that a given system variable P is adjusted to a desired value at the final time t .

C. Spectral overlap

Alternatively, Eq. (11) can be written as an overlap of system-and bath matrices, which allows a more direct physical interpretation. To do so, we assume d dimensional Hilbert-space, and expand the interaction Hamiltonian as a sum of products of system and bath operators,

$$\hat{H}_I = \sum_{j=1}^{d^2-1} \hat{S}_j \otimes \hat{B}_j, \quad (12)$$

in such a way that $\langle \hat{B}_j \rangle = 0$, which ensures that Eq. (9) is satisfied (otherwise we may shift $\hat{B}'_j = \hat{B}_j - \langle \hat{B}_j \rangle \hat{I}$, $\hat{H}'_S = \hat{H}_S + \sum_j \langle \hat{B}_j \rangle \hat{S}_j$). Considering Eq. (12) in the interaction picture and expanding $\hat{S}_j(t) = \sum_k \epsilon_{jk}(t) \hat{S}_k$ in terms of [Hermitian, traceless, orthonormalized to $\text{Tr}(\hat{S}_j \hat{S}_k) = d \delta_{jk}$] basis operators \hat{S}_j , defines a (real orthogonal) rotation matrix $\epsilon(t)$ in the system's Hilbert space, with elements

$$\epsilon_{jk}(t) = \langle \hat{S}_j(t) \hat{S}_k \rangle_{\text{id}}, \quad (13)$$

where $\langle \cdot \rangle_{\text{id}} = \text{Tr}[d^{-1} \hat{I}(\cdot)]$. These elements of the matrix $\epsilon(t)$ may be regarded as the dynamical correlation functions of the basis operators. Analogously, we define a

bath correlation matrix $\Phi(t)$ with elements

$$\Phi_{jk}(t) = \langle \hat{B}_j(t) \hat{B}_k \rangle_{\text{B}}. \quad (14)$$

It contains the entire description of the bath behavior in our approximation. Finally, we define a Hermitian matrix Γ with elements

$$\Gamma_{kj} = \langle [\hat{S}_j, \hat{P}] \hat{S}_k \rangle, \quad (15)$$

where $\langle \cdot \rangle = \text{Tr}[\hat{\rho}(0)(\cdot)]$. The matrix Γ may be understood as a representation of the gradient \hat{P} with respect to the chosen basis operators \hat{S}_j . Finally, we define the bath and (finite-time) system spectra according to

$$\mathbf{G}(\omega) = \int_{-\infty}^{\infty} dt e^{i\omega t} \Phi(t), \quad (16)$$

$$\epsilon_t(\omega) = \frac{1}{\sqrt{2\pi}} \int_0^t d\tau e^{i\omega\tau} \epsilon(\tau). \quad (17)$$

This allows to express the score, Eq. (11), as the matrix overlap

$$P = \iint_0^t dt_1 dt_2 \text{Tr}[\epsilon^\dagger(t_1) \Phi(t_1 - t_2) \epsilon(t_2) \Gamma] \quad (18)$$

$$= \int_{-\infty}^{\infty} d\omega \text{Tr}[\epsilon_t^\dagger(\omega) \mathbf{G}(\omega) \epsilon_t(\omega) \Gamma] \quad (19)$$

$$= t \int_{-\infty}^{\infty} d\omega \text{Tr}[\mathbf{F}_t(\omega) \mathbf{G}(\omega)]. \quad (20)$$

In Eq. (20) we have used the cyclic property of the trace to write the spectral overlap in a more compact form by combining the rotation matrix spectra $\epsilon_t(\omega)$ and the gradient representation Γ to a system spectral matrix

$$\mathbf{F}_t(\omega) = \frac{1}{t} \epsilon_t(\omega) \Gamma \epsilon_t^\dagger(\omega). \quad (21)$$

Analogously, Eq. (18) can be written in a more compact form by introducing the matrix

$$\mathbf{R}(t_1, t_2) = \epsilon^\dagger(t_1) \Phi(t_1 - t_2) \epsilon(t_2). \quad (22)$$

Equation (20) is as a generalization of Kofman and Kurizki [35] and demonstrates that the change P over a given time t is determined by the spectral overlap between system and bath dynamics, analogously to DCM [13], or the measurement induced quantum Zeno and anti-Zeno control of open systems [21, 36]. The bath-spectral matrix $\mathbf{G}(\omega)$ must be positive semi-definite for all ω . If the same holds for the matrix $\mathbf{F}_t(\omega)$, then P is always positive. Below we will consider such a case where P reflects a gate error and the goal is then to minimize this error. The spectral overlap Eq. (20) can be made as small as desired by a rapid modulation of the system, such that the entire weight of the system spectrum is shifted beyond that of the bath, which is assumed to vanish for sufficiently high frequencies. Since this fast modulation may cause unbounded growth of the system

energy, a meaningful posing of the problem requires a constraint.

In general, $\mathbf{F}_t(\omega)$ is Hermitian but need not necessarily be positive semi-definite, depending on the choice of score as encoded in Γ . This reflects the fact that P can increase or decrease over t . Depending on the application, our goal can therefore also be to maximize P with positive and negative sign. In what follows we will consider the question how to find a system dynamics that optimizes the score.

III. EULER-LAGRANGE OPTIMIZATION

A. Role of control, score and constraint

Our considerations in the previous section suggest to define our control problem in terms of a triple (\mathbf{f}, P, E) consisting of a control \mathbf{f} , a score P , and a constraint E .

The *control* is a set of real parameters f_l , which have been combined to a vector \mathbf{f} . These can either be timings, amplitudes, and/or phases of a given number of discrete pulses, or describe a time-continuous modulation of the system. Here, we focus on time-dependent control, where the $f_l(\tau)$ parametrize the system Hamiltonian as $\hat{H}_S = \hat{H}_S[\mathbf{f}(\tau)]$, or the unitary evolution operator $\hat{U}(\tau) = T_+ e^{-i \int_0^\tau d\tau' \hat{H}_S(\tau')} \equiv \hat{U}[\mathbf{f}(\tau)]$. A direct parametrization of \hat{U} avoids the need of time-ordered integration of its exponent. The $\hat{U}(\tau)$ thus obtained [37] can be then used to calculate the system Hamiltonian $\hat{H}_S(\tau) = i[\frac{\partial}{\partial t} \hat{U}(\tau)] \hat{U}^\dagger(\tau)$.

Two explicit examples of the score P pertain to the fidelity of \hat{P} with a given pure state $F_\Psi = \langle \Psi | \hat{\rho} | \Psi \rangle$, (for which $\hat{P} = |\Psi\rangle\langle\Psi|$), or to the von Neumann entropy which we can approximate (for nearly pure states) by the linear entropy, $S = -k \text{Tr}(\hat{\rho} \ln \hat{\rho}) \approx S_L = k[1 - \text{Tr}(\hat{\rho}^2)]$, [for which $\hat{P} = -2k\hat{\rho}(0)$]. The latter score can be used to maximize the fidelity with the maximally mixed state $\hat{\rho} \sim \hat{I}$ (for which S_L becomes maximum), or to maximize the concurrence $C_{|\Psi_{AB}\rangle} = \sqrt{2(1 - \text{Tr} \hat{\rho}_A^2)}$, $\hat{\rho}_A = \text{Tr}_B |\Psi_{AB}\rangle\langle\Psi_{AB}|$, as a measure of entanglement of a pure state $|\Psi_{AB}\rangle$ of a bipartite system.

If a *constraint* is required to ensure the existence of a finite (physical) solution, its choice should depend on the most critical source of error. An example is the average speed with which the controls change, $E = \int_0^t d\tau \dot{\mathbf{f}}^2(\tau)$, which depend on the control bandwidth in the spectral domain. A parametrization-independent alternative is the mean square of the modulation energy, $E = \int_0^t d\tau \langle (\Delta \hat{H})^2(\tau) \rangle_{\text{id}}$, where $\langle \cdot \rangle_{\text{id}}$ refers to a maximally mixed state and hence to a state-independent norm, and $\Delta \hat{H}$ is the difference between the modulated and unmodulated (natural) system Hamiltonians.

B. A projected gradient search

We want to find controls \mathbf{f} that optimize a score $P(\mathbf{f})$ subject to a constraint $E(\mathbf{f})$. A numerical local optimization can be visualized in parameter space as shown in Fig. 2.

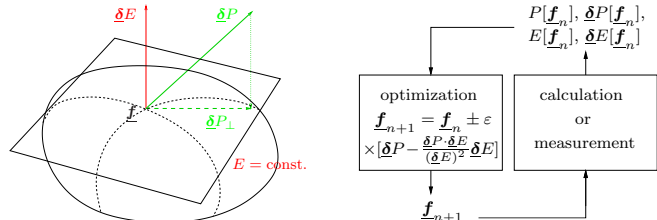


FIG. 2: Left: Optimization of the score $P(\mathbf{f})$ subject to a constraint $E(\mathbf{f})$ in control space $\{\mathbf{f}\}$ by walking along the component δP_\perp of the gradient δP orthogonal to δE . Right: Resulting iteration consisting in steps determined by a small parameter ϵ which yields a local solution depending on the starting point \mathbf{f}_0 .

We start at some initial point \mathbf{f}_0 for which $E(\mathbf{f}_0)$ is the desired value of the constraint. Simply following the gradient δP would maximize or minimize P , but also change E . To optimize P while keeping E constant, we therefore move along the projection of δP orthogonal to δE , i.e., along $\delta P_\perp = \delta P - \frac{\delta P \cdot \delta E}{(\delta E)^2} \delta E$. Since the gradients depend on \mathbf{f} , the iteration consists of small steps $\mathbf{f}_{n+1} = \mathbf{f}_n \pm \epsilon \delta P_\perp(\mathbf{f}_n)$, $\epsilon \ll 1$. Assuming that neither δP nor δE vanish, the iteration will come to a halt where δP_\perp vanishes, because the gradients are parallel,

$$\delta P = \lambda \delta E. \quad (23)$$

This condition constitutes the Euler-Lagrange (EL) equation of the extremal problem, with the proportionality constant λ being the Lagrange multiplier. Its concrete form depends on the choice of P and E . Since the solutions of the EL optimization represent local optima of the constrained P , we may repeat the search with randomly chosen \mathbf{f}_0 a number of times and select the best solution. The gradients at each point \mathbf{f}_n may be obtained either from a calculation based on prior knowledge of the bath or experimentally from data measured in real time. A discretization of the time interval $0 \leq \tau \leq t$ then reduces the variational δ to a finite-dimensional vector gradient ∇ .

IV. GATE PROTECTION WITH BOMECS

A. Gate error as average fidelity decline

A particular application of our formalism is decoherence protection of a given quantum operation by bath-optimal minimal-energy control (BOMECS) [13, 37]. Consider the implementation of a predetermined quantum

gate, i.e., unitary operation within a given ‘‘gate time’’ t . It is sufficient to consider a pure input state $|\Psi\rangle$. In the interaction picture with respect to the desired gate operation and in the absence of bath effects, we should therefore observe at time t the initial state $|\Psi\rangle$. The quantity of interest is here the fidelity $\langle\Psi|\hat{\rho}(t)|\Psi\rangle$, and we use the projector $\hat{P} = \hat{\rho}(0) = |\Psi\rangle\langle\Psi|$ as the gradient operator, so that Eq. (10) is satisfied and Eq. (11) gives the fidelity change as the score

$$P = \langle\Psi|\Delta\hat{\rho}|\Psi\rangle = -t^2\langle\Psi|\hat{H}^2|\Psi\rangle - \langle\Psi|\hat{H}|\Psi\rangle^2, \quad (24)$$

which is given by \hat{H} defined in Eq. (11).

Since a quantum gate is supposed to act on an unknown input state, we need to get rid of the dependence on $|\Psi\rangle$. One possibility is to perform a uniform average over all $|\Psi\rangle$. We may apply

$$\overline{\langle\Psi|\hat{A}|\Psi\rangle\langle\Psi|\hat{B}|\Psi\rangle} = \frac{\text{Tr}\hat{A}\hat{B} + \text{Tr}\hat{A}\text{Tr}\hat{B}}{d(d+1)} \quad (25)$$

[38, 39] which gives the average

$$\overline{P} = -t^2 \frac{d}{d+1} \langle\hat{H}^2\rangle_{\text{id}}, \quad (26)$$

where $\langle\cdot\rangle_{\text{id}} = \text{Tr}[d^{-1}\hat{I} \otimes \hat{\rho}_{\text{B}}(\cdot)]$. In Eq. (26) we have used $\text{Tr}_{\text{S}}\hat{H} = \hat{0}$, which corresponds to $\text{Tr}\hat{S}_j = 0$ in Sec. II C. Because of this and because of Eq. (9), $\langle\hat{H}\rangle_{\text{B}} = \langle\hat{H}_1\rangle_{\text{B}} = \hat{0}$, we have $\langle\hat{H}\rangle_{\text{id}} = 0$, and Eq. (26) also describes the variance $\text{Var}(\hat{H}) = \langle\hat{H}^2\rangle_{\text{id}} - \langle\hat{H}\rangle_{\text{id}}^2$. On the other hand $\hat{P} = -2k\hat{\rho}(0)$ that gives the change ΔS of entropy $S = -k\text{Tr}(\hat{\rho}\ln\hat{\rho})$ is (up to a proportionality factor of $-2k$) the same as the \hat{P} used here to give the change of fidelity, we have $\Delta S = -2kP$. If we define a *gate error* \mathcal{E} as the average fidelity decline, $\mathcal{E} = -\overline{P}$, with \overline{P} given in Eq. (26), we can summarize the following proportionalities: gate error \equiv average fidelity decline \sim average entropy increase (purity decline) $\Delta S \sim$ square (variance) of the average interaction energy \hat{H} :

$$\mathcal{E} \equiv -\overline{P} = \frac{\overline{\Delta S}}{2k} = t^2 \frac{d}{d+1} \langle\hat{H}^2\rangle_{\text{id}} = t^2 \frac{d}{d+1} \text{Var}(\hat{H}). \quad (27)$$

In the matrix representation of Sec. II C, the average over the initial states in the matrix $\mathbf{\Gamma}$ defined in Eq. (15), gives $\overline{\mathbf{\Gamma}} = -\frac{d}{d+1}\mathbf{I}$ [using $\text{Tr}(\hat{S}_j\hat{S}_k) = d\delta_{jk}$ and $\text{Tr}\hat{S}_j = 0$], so that

$$\mathcal{E} = \frac{d}{d+1} \int_{-\infty}^{\infty} d\omega \text{Tr}[\epsilon_t(\omega)\epsilon_t^\dagger(\omega)\mathbf{G}(\omega)] \quad (28)$$

in agreement with [37] [except a different normalization $\text{Tr}(\hat{S}_j\hat{S}_k) = 2\delta_{jk}$ leading there to a prefactor $\frac{2}{d+1}$]. From the requirement that $\mathcal{E} \geq 0$ must hold for any positive semi-definite matrix $\epsilon_t(\omega)\epsilon_t^\dagger(\omega)$, we conclude that $\mathbf{G}(\omega)$ must be a positive semi-definite matrix for any ω . The task of BOMECE is then to find a system evolution $\hat{U}(\tau)$ (cf. the control examples in the previous section) that minimizes \mathcal{E} , subject to the boundary condition that the final $\hat{U}(t)$ is the desired gate.

B. Comparison of BOMECE with DD

It is appropriate to compare the effect of dynamical decoupling (DD) [5, 6] with that of BOMECE. DD does not change with the bath spectrum $\mathbf{G}(\omega)$. With an increasing number of pulses, DD shifts the weight of the system spectrum $F(\omega)$ towards higher frequencies, until the overlap Eq. (20) has become sufficiently small. This is illustrated for two different numbers of pulses of periodic DD (PDD, pulses periodic in time), in the upper row of Fig. 3 in the case of a 1D single qubit modulation (i.e., all pulses are given by an arbitrary but fixed Pauli matrix).

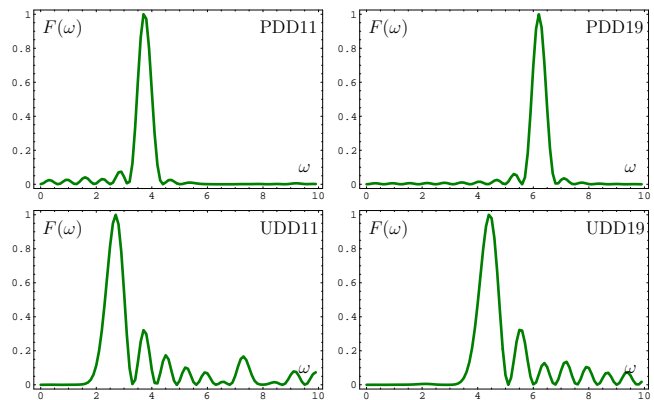


FIG. 3: System modulation spectra $F(\omega)$ generated by two methods of DD. Upper row: periodic dynamical decoupling with n π -pulses (PDD n), lower row: Uhrig dynamical decoupling with the same number of π -pulses (UDD n), compared for $n = 11$ (left column) and $n = 19$ (right column) pulses.

Aperiodic DD such as UDD [6] suppress low-frequency components (to the left of the main peak) in the system spectrum, which retain the system-bath coupling even if the main peak of the system spectrum has been shifted beyond the bath cutoff frequency (Fig. 3). The plots indicate that this suppression of low frequency components is achieved at the price of a smaller shift of the main peak, i.e., shifting the main peak beyond a given cutoff requires more pulses in UDD than in PDD. Note that optimized DD sequences with improved asymptotics exist [7], which we will not consider here.

System modulation spectra obtained with BOMECE are shown in Fig. 4.

The plot refers to a qubit subject to pure dephasing (i.e., Z -coupling) by a bath whose spectrum $G(\omega)$ has a Lorentzian peak and low-frequency tail. The BOMECE optimizes $\hat{U}(\tau)$ simultaneously for 3D Pauli matrix couplings to the bath (Z , Y and X). The resulting system spectrum $F(\omega)$ is shown for different energy constraints E which are increased in small and equal steps. For low E , $F(\omega)$ has a single peak on the left of the bath peak. Increasing E causes a second peak of $F(\omega)$ to emerge on the right of the bath peak, which continues to grow, while the peak on the left diminishes, until for high E , only the

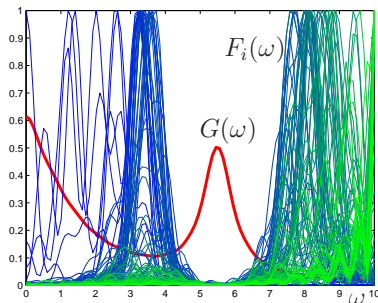


FIG. 4: BOMEK-minimization of the gate error for a single qubit π -gate caused by pure dephasing with a given bath spectrum [$G(\omega)$, bold red line]. The Z -components of the obtained system modulation spectra $F_i(\omega)$ are shown for energy constraints $E_i = 0.1 + 4(i - 1)$, $i = 1, 2, \dots, 101$, (thin lines, blue to green) individually scaled to 1.

right peak remains. Fig. 4 hence demonstrates that the spectrum $F(\omega)$ generated by BOMEK changes continuously as E increases, but avoids overlap with the maxima of $G(\omega)$ irrespective of E . BOMEK can therefore be superior to all forms of DD including UDD, especially if the bath has high cutoff but bandgaps at low frequencies.

V. PURITY CONTROL OF A QUBIT

To give an example of the opposite case, where the goal is to maximize the system-bath coupling, we apply our approach of constrained optimization to the linear entropy $S_L = 2[1 - \text{Tr}(\hat{\rho}^2)]$ of a qubit. [Note that here S_L has been normalized to 1 by setting the coefficient $k = d/(d - 1) = 2$, cf. Sec. III.] We assume an initial mixture

$$\hat{\rho}(0) = p|1\rangle\langle 1| + (1 - p)|0\rangle\langle 0| \quad (29)$$

of a ground (excited) state $|0\rangle$ ($|1\rangle$), where $0 \leq p \leq 0.5$ is related to S_L by $p = (1 - \sqrt{1 - S_L})/2$. With $\hat{S}_j = \hat{\sigma}_j$ denoting for $d = 2$ the Pauli matrices, Eq. (29) can be written in terms of $\hat{H}_0 = \frac{\omega_0}{2}\hat{\sigma}_3$ as $\hat{\rho}(0) = \frac{e^{-\beta\hat{H}_0}}{\text{Tr}(e^{-\beta\hat{H}_0})} = \frac{|1\rangle\langle 1|}{1 + e^{\beta\omega_0}} + \frac{|0\rangle\langle 0|}{1 + e^{-\beta\omega_0}}$, where $\beta = \frac{\ln(p^{-1} - 1)}{\omega_0}$ is the inverse temperature. Purity and temperature are hence related via the energy scale ω_0 . Our goal is a constrained optimization of ΔS_L , i.e., $\dot{P} = -4\hat{\rho}(0)$ in Eq. (2). Unlike the gate error Eq. (27), ΔS_L can be negative or positive, which can be understood as cooling or heating, respectively.

The time evolutions resulting from a minimization of ΔS_L for the initial state Eq. (29) are illustrated in Fig. 5. The f_j shown in Fig. 5(a) are defined by $\hat{U}(\tau) = e^{-\frac{1}{2}f_3(\tau)\hat{\sigma}_3} e^{-\frac{1}{2}f_2(\tau)\hat{\sigma}_2} e^{-\frac{1}{2}f_1(\tau)\hat{\sigma}_1}$, whereas the ω_j shown in Fig. 5(b) are given by $\hat{H}_S(\tau) = \sum_j \omega_j(\tau)\hat{\sigma}_j$. The chosen constraint $E = \frac{1}{2} \int_0^t d\tau \text{Tr}(H_S - \hat{H}_0)^2(\tau)$ can be written in terms of the f_j as $E = \frac{1}{4} \int_0^t dt_1 [f_1^2 + f_2^2 + (\dot{f}_3 - \omega_0)^2 + 2\dot{f}_1(\dot{f}_3 - \omega_0) \cos f_2]$. The overlap between the evolving

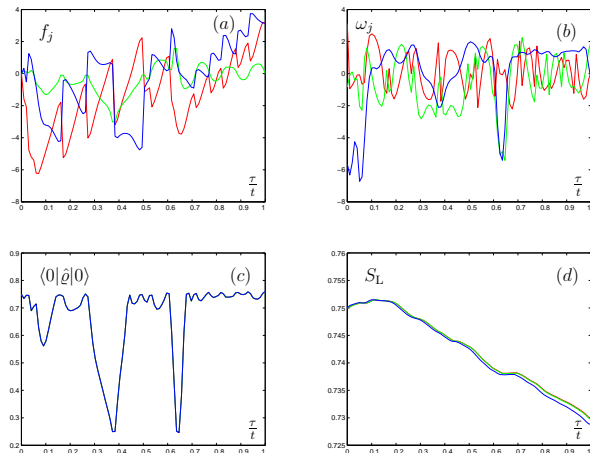


FIG. 5: Evolution within $0 \leq \tau \leq t$ for an optimized cooling with initial $p = 0.25$ of (a) effective and (b) instantaneous controls (red, green, and blue graphs show x , y , and z component), (c) ground state overlap of the system state, and (d) linear entropy [green, red and blue graph show numerical integration of the Nakajima-Zwanzig equation, time-convolutionless equation, and second order approximation of the solution [1], which are indistinguishable in (c)] (system-bath coupling strength $\kappa = 10^{-2}$, $\omega_0 = \frac{2\pi}{t}$, $t = 10$, $E = 100$).

system state $\hat{\rho}(\tau)$ (in the Schrödinger picture) and the ground state $|0\rangle$ shown in Fig. 5(c) indicates the fast unitary system modulation through short time population inversions without significantly altering the state purity as verified in Fig. 5(d). This can be visualized as fast π -rotations of the state inside the Bloch sphere, which, together with smaller rotations, here result in the final reduction of $S_L(t)$ seen in Fig. 5(d). Fig. 5(d) also confirms that for the chosen time and coupling strength, differences between various methods of approximation are small.

In contrast to gate protection, no initial-state averaging is performed here, i.e., Eq. (29) is known. Consequently, as Fig. 6 shows, the relevant components $F_j \equiv (\mathbf{F}_t)_{jj}(\omega)$ of the system modulation spectrum contributing to the spectral overlap Eq. (20) depend on the initial state $\hat{\rho}(0)$ via the matrix $\mathbf{\Gamma}$ Eq. (15). [We assume an uncorrelated bath, i.e., $G_{jk}(\omega) = 0$ for $j \neq k$ and $G_j \equiv G_{jj}(\omega)$.] This influence is clearly visible in case of a constant (unmodulated, i.e., free) Hamiltonian (middle column), for which we set $\omega_0 = \frac{2\pi}{t}$ with the final t being in the order of the bath correlation time. Cooling (heating) is achieved by realizing negative (positive) ΔS_L via maximum negative (positive) spectral overlap, as shown in the left (right) column of Fig. 6. This is the opposite to system-bath decoupling, where the goal is to minimize the overlap.

The plots illustrate the role of the energy constraint E : increasing E allows to establish overlap with higher frequency components of the bath spectrum. This also suggests that for a bath spectrum with a finite frequency

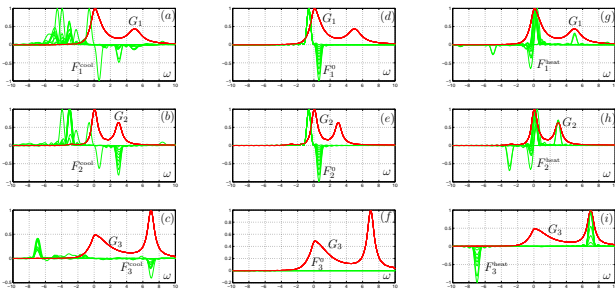


FIG. 6: Cooling and heating of a TLS by minimization (left: a, b, c) and maximization (right: g, h, i) of the change of linear entropy for a given bath spectrum (red, G_j) with $j = 1, 2, 3$ denoting x, y and z component. The optimized system spectra (F_j , green) are shown for an energy constraint $E = 10^2$ (left) and $E = 10^3$ (right) as contrasted to the unmodulated Hamiltonian \hat{H}_0 (i.e., for $E = 0$, middle: d, e, f) and different initial states with $p = 0.001, 0.05, 0.1, \dots, 0.45, 0.499$.

cutoff, increasing E beyond a certain saturation value will not lead to further improvement of the optimization, cf. the general considerations in App. A. In the time domain, increasing E leads to more rapid changes in the physical Hamiltonian however, requiring higher resolution of the numerical treatment. On the contrary, for attempted cooling (heating) by minimization (maximization) of ΔS_L , a given E may be too small to lead to negative (positive) ΔS_L . The obtained ΔS_L may then be understood as “reduced heating” (“reduced cooling”) as compared to a ΔS_L obtained with an unmodulated \hat{H}_0 . This is shown in Fig. 7. The figure also illustrates

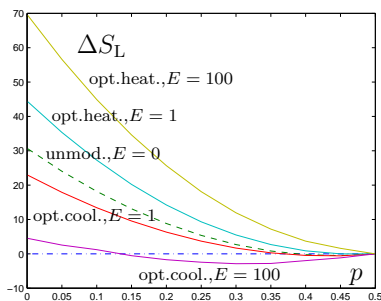


FIG. 7: Change of linear entropy in units of the system-bath coupling strength obtained by minimization (attempted cooling) and maximization (attempted heating) of ΔS_L under different constraints $E = 0, 1, 100$ as a function of the initial p for a bath as shown in Fig. 6.

once more that the $\hat{\varrho}(0)$ -dependence of the spectra shown in Fig. 6 is accompanied by a $\hat{\varrho}(0)$ -dependency of the achievable change ΔS_L for a given bath. For a maximally mixed state in particular ($p = 0.5$), the matrix $\mathbf{\Gamma}$ Eq. (15) vanishes and with it ΔS_L .

A possibility to achieve negative (positive) ΔS_L by its

minimization (maximization) even for weak modulation (i.e., for small E), is to adapt the temperature of the bath such that for an undriven system Hamiltonian \hat{H}_0 , no change is observed, $\Delta S_L = 0$, which is a necessary condition for a system-bath equilibrium. This is would require non-unitary system modulation, e.g., the effect of repeated measurements [40–42].

VI. SUMMARY AND OUTLOOK

Peculiarity of the approach: In summary, we have considered a way of finding a time-dependence of the system Hamiltonian over a fixed time interval such that a given system observable attains a desired value at the end of this interval. The peculiarity of our approach is that it relies on knowledge of the bath coupling spectrum and adapts the spectrum of the system modulation to it. This allows to adjust the modulation to bandgaps or peaks in the bath coupling spectrum. In contrast to dynamic decoupling of system and bath, which can be achieved by shifting the entire system-modulation spectrum beyond some assumed bath cutoff frequency, an enhancement of the coupling requires more detailed knowledge on the peak positions of the bath spectrum. In this way, our approach may comprise suppression and enhancement of the system-bath coupling in a unified way for executing more general tasks than decoherence suppression. The same approach can also be applied to map out the bath spectrum by measuring the coherence decay rate for a narrow-band modulation centered at different frequencies [43].

As far as the controls are concerned, we here consider time-continuous modulation of the system Hamiltonian, which allows for vastly more freedom compared to control that is restricted to stroboscopic pulses as in DD [5–7]. We do not rely on rapidly changing control fields that are required to approximate stroboscopic π -pulses. These features allow efficient optimization under energy constraint. On the other hand, the generation of a sequence of well-defined pulses may be preferable experimentally. We may choose the pulse timings and/or areas as continuous control-parameters and optimize them with respect to a given bath spectrum. Hence, our approach encompasses both pulsed and continuous modulation as special cases.

Open issues: An open issue of the approach is the inclusion of higher orders in the system-bath coupling, which becomes important for strong or resonant system-bath coupling, so that a perturbative expansion cannot be applied. This may be the case especially when this coupling is to be enhanced in order to achieve a non-unitary operation (e.g. cooling), since in this case an optimization of the coupling may take us out of the domain of validity of the entire approach.

Another concern regards the initial conditions. Here we have assumed a factorized initial state of the system and bath. This prevents us from taking into account

system-bath-interactions that may have occurred prior to that time. In particular, if the system is in equilibrium with the bath, their states are entangled or correlated [17, 40].

An immediate problem of both higher order coupling and system-bath correlations is that their consideration requires knowledge of the corresponding parameters. It may be difficult to obtain such data with sufficient experimental precision. Moreover, its consideration renders the theory cumbersome and the intuition gained from the spectral overlap approach presented here is lost. A way out is offered by replacing the “open” iteration loop in Fig. 2 with a “closed” loop [44], where the calculation of the score, constraint and their gradients are based on actual measurements performed on the controlled system in real time rather than on prior model assumptions, i.e., knowledge of bath properties. Such closed loop control would allow efficient optimization, but at the cost of losing any insight into the physical mechanisms behind the result obtained.

From a fundamental point of view, it is interesting to derive analytic bounds of a desired score (under a chosen constraint) and see if this bound can be achieved by means of some (global) optimization, i.e., if the bound is tight. The need for a constraint in such optimization is not obvious if the task requires coupling enhancement, especially when the bath spectrum has a single maximum (Appendix A).

Acknowledgments

The support of the EU (FET Open Project MIDAS), ISF and DIP is acknowledged

Appendix A: Bound estimation

Our goal is to give constraint-independent upper and lower bounds for the maximum change $P = \text{Tr}(\hat{P}\Delta\hat{\rho})$ that can be achieved with a given bath and \hat{P} under the condition (10). We assume that ϵ , $\mathbf{\Gamma}$, and $\mathbf{G}(\omega)$ are quadratic $(d^2 - 1)$ -dimensional matrices. If $\max[\text{Tr}\mathbf{G}(\omega)] < \infty$, we can estimate P by using that $\text{Tr}(\mathbf{A}\mathbf{B}) \leq \text{Tr}(\mathbf{A})\text{Tr}(\mathbf{B})$ for positive semi-definite matrices \mathbf{A} , \mathbf{B} , and applying Hölder’s inequality in the form of $\int_{-\infty}^{\infty} d\omega |f(\omega)g(\omega)| \leq$

$\sup\{|g(\omega)|\} \int_{-\infty}^{\infty} d\omega |f(\omega)|$. Decomposing $\mathbf{\Gamma} = \mathbf{\Gamma}_1 - \mathbf{\Gamma}_2$ into positive semi-definite matrices $\mathbf{\Gamma}_i$ and making use of $\frac{1}{t} \int_{-\infty}^{\infty} d\omega \epsilon_t^\dagger(\omega)\epsilon_t(\omega) = \hat{I}$ we thus get

$$-P_2 \leq P \leq P_1, \quad P_i = t \sup[\text{Tr}\mathbf{G}(\omega)] \text{Tr}\mathbf{\Gamma}_i. \quad (\text{A1})$$

This reveals that for given t and $\mathbf{G}(\omega)$, the bounds P_i depend on $\hat{\rho}(0)$ and \hat{P} via $\mathbf{\Gamma}$.

Appendix B: Non-commuting score

If Eq. (10) does not hold, the following modifications must be made. We denote by $\mathbf{A}_\pm = (\mathbf{A} \pm \mathbf{A}^\dagger)/2$ the (skew) Hermitian part of a given matrix $\mathbf{A} = \mathbf{A}_+ + \mathbf{A}_-$ for convenience. Equation (11) must be replaced with

$$\begin{aligned} \tilde{P} &= 2\text{Re} \int_0^t dt_1 \int_0^{t_1} dt_2 \langle [\hat{H}_1(t_1), \hat{P}] \hat{H}_1(t_2) \rangle \quad (\text{B1}) \\ &= P + \int_0^t dt_1 \int_0^{t_1} dt_2 \text{Tr}\{[\hat{\rho}_{\text{tot}}(0), \hat{P}] \hat{H}_1(t_2) \hat{H}_1(t_1)\}, \quad (\text{B2}) \end{aligned}$$

where $\langle \cdot \rangle = \text{Tr}[\hat{\rho}_{\text{tot}}(0)(\cdot)]$ and P is defined in Eq. (11). Equivalently, we can write

$$\tilde{P} = 2 \int_0^t dt_1 \int_0^{t_1} dt_2 \text{Tr}[\mathbf{R}_+(t_1, t_2) \mathbf{\Gamma}_+ + \mathbf{R}_-(t_1, t_2) \mathbf{\Gamma}_-] \quad (\text{B3})$$

$$= P - 2 \int_0^t dt_1 \int_0^{t_1} dt_2 \text{Tr}[\mathbf{R}^\dagger(t_1, t_2) \mathbf{\Gamma}_-], \quad (\text{B4})$$

where P is given by Eq. (18) together with Eq. (22). In the spectral domain, the analogous expression is

$$\tilde{P} = 2t \text{Re} \int_{-\infty}^{\infty} d\omega \text{Tr}[\mathbf{F}_t(\omega) \mathbf{G}(\omega)] \quad (\text{B5})$$

$$= P - 2t \int_{-\infty}^{\infty} d\omega \text{Tr}[\mathbf{F}_-(\omega) \mathbf{G}^\dagger(\omega)], \quad (\text{B6})$$

where P is given in Eq. (20) and

$$\mathbf{G}(\omega) = \int_0^\infty dt e^{i\omega t} \mathbf{\Phi}(t), \quad (\text{B7})$$

is related to Eq. (16) by $\mathbf{G}(\omega) = 2\mathbf{G}_+(\omega)$.

-
- [1] H.-P. Breuer and F. Petruccione, *The Theory of Open Quantum Systems* (Oxford University Press, Oxford, 2002).
- [2] N. Bar-Gill and G. Kurizki, Phys. Rev. Lett. **97**, 230402 (2006).
- [3] L.-A. Wu, G. Kurizki, and P. Brumer, Phys. Rev. Lett. **102**, 080405 (2009).
- [4] M. A. Nielsen and I. L. Chuang, *Quantum Computation and Quantum Information* (Cambridge University Press, Cambridge, 2000).
- [5] L. Viola, E. Knill, and S. Lloyd, Phys. Rev. Lett. **82**, 2417 (1999).
- [6] G. S. Uhrig, Phys. Rev. Lett. **98**, 100504 (2007).
- [7] W.-J. Kuo and D. A. Lidar (2011), <http://arxiv.org/abs/1106.2151>.
- [8] J.-M. Cai, F. Jelezko, M. B. Plenio, and A. Retzker (2011), <http://arxiv.org/abs/1111.0930>.
- [9] A. G. Kofman and G. Kurizki, Phys. Rev. Lett. **87**,

- 270405 (2001).
- [10] A. Barone, G. Kurizki, and A. G. Kofman, Phys. Rev. Lett. **92**, 200403 (2004).
- [11] A. G. Kofman and G. Kurizki, Phys. Rev. Lett. **93**, 130406 (2004).
- [12] G. Gordon, N. Erez, and G. Kurizki, J. Phys. B: At. Mol. Opt. Phys. **40**, S75 (2007).
- [13] G. Gordon, G. Kurizki, and D. A. Lidar, Phys. Rev. Lett. **101**, 010403 (2008).
- [14] R. Alicki, J. Phys. A **12**, L103 (1979).
- [15] G. Lindblad, *Non-Equilibrium Entropy and Irreversibility* (D. Reidel, Holland, 1983); J. Gemmer, M. Michel, and G. Mahler, *Quantum Thermodynamics: Emergence of Thermodynamic Behavior Within Composite Quantum Systems*, vol. 657 of *Lecture Notes in Physics* (Springer, Berlin Heidelberg, 2004); R. Alicki, M. Horodecki, P. Horodecki, and R. Horodecki, Open Systems and Information Dynamics **11**, 205 (2004), ISSN 1230-1612, 10.1023/B:OPSY.0000047566.72717.71; H. Spohn, J. Math. Phys. **19**, 1227 (1978); J. Gemmer, A. Otte, and G. Mahler, Phys. Rev. Lett. **86**, 1927 (2001).
- [16] G. Gordon, G. Bensky, D. Gelbwaser-Klimovsky, D. Rao, N. Erez, and G. Kurizki, New J. Phys. **11**, 123025 (2009).
- [17] G. Gordon, D. D. B. Rao, and G. Kurizki, New Journal of Physics **12**, 053033 (2010).
- [18] G. A. Álvarez, D. D. B. Rao, L. Frydman, and G. Kurizki, Phys. Rev. Lett. **105**, 160401 (2010).
- [19] J. Chan, T. P. M. Alegre, A. H. Safavi-Naeini, J. T. Hill, A. Krause, S. Gröblacher, M. Aspelmeyer, and O. Painter, Nature **478**, 89 (2011).
- [20] G. Harel, G. Kurizki, J. K. McIver, and E. Coutsias, Phys. Rev. A **53**, 4534 (1996); B. M. Garraway, B. Sherman, H. Moya-Cessa, P. L. Knight, and G. Kurizki, Phys. Rev. A **49**, 535 (1994).
- [21] A. G. Kofman and G. Kurizki, Nature (London) **405**, 546 (2000).
- [22] T. Opatrný, G. Kurizki, and D.-G. Welsch, Phys. Rev. A **61**, 032302 (2000).
- [23] M. O. Scully, M. S. Zubairy, G. S. Agarwal, and H. Walther, Science **299**, 862 (2003); M. O. Scully, Phys. Rev. Lett. **88**, 050602 (2002); M. O. Scully, Phys. Rev. Lett. **104**, 207701 (2010); M. O. Scully, K. R. Chapin, K. E. Dorfman, M. B. Kim, and A. Svidzinsky, Proceedings of the National Academy of Sciences (2011), <http://www.pnas.org/content/early/2011/08/25/1110234108.full.pdf+html>; T. Opatrný, American Journal of Physics **73**, 63 (2005).
- [24] R. van Grondelle and V. I. Novoderezhkin, Nature **463**, 614 (2010).
- [25] G. D. Scholes, Nature Physics **7**, 448 (2011).
- [26] R. D. Schaller and V. I. Klimov, Phys. Rev. Lett. **92**, 186601 (2004); R. D. Schaller, M. Sykora, J. M. Pietryga, and V. I. Klimov, Nano Lett. **6**, 424 (2006).
- [27] R. E. Blankenship, D. M. Tiede, J. Barber, G. W. Brudvig, G. Fleming, M. Ghirardi, M. R. Gunner, W. Junge, D. M. Kramer, A. Melis, et al., Science **332**, 805 (2011).
- [28] B. M. Escher, G. Bensky, J. Clausen, and G. Kurizki, J. Phys. B: At. Mol. Opt. Phys. **44**, 154015 (2011).
- [29] K. G. H. Vollbrecht, C. A. Muschik, and J. I. Cirac, Phys. Rev. Lett. **107**, 120502 (2011).
- [30] D. D. Bhaktavatsala Rao, N. Bar-Gill, and G. Kurizki, Phys. Rev. Lett. **106**, 010404 (2011); D. Braun, Phys. Rev. Lett. **89**, 277901 (2002); G. Kurizki, Phys. Rev. A **42**, 2915 (1990); G. Kurizki, A. G. Kofman, and V. Yudson, Phys. Rev. A **53**, R35 (1996).
- [31] G. Gordon and G. Kurizki, Phys. Rev. Lett. **97**, 110503 (2006).
- [32] J. Cai, G. G. Guerreschi, and H. J. Briegel, Phys. Rev. Lett. **104**, 220502 (2010).
- [33] T. Scholak, F. de Melo, T. Wellens, F. Mintert, and A. Buchleitner, Phys. Rev. E **83**, 021912 (2011).
- [34] A. N. Pechen and D. J. Tannor, Phys. Rev. Lett. **106**, 120402 (2011).
- [35] A. G. Kofman and G. Kurizki, IEEE Trans. Nanotechnology **4**, 116 (2005).
- [36] A. G. Kofman and G. Kurizki, Phys. Rev. A **54**, R3750 (1996).
- [37] J. Clausen, G. Bensky, and G. Kurizki, Phys. Rev. Lett. **104**, 040401 (2010).
- [38] C. Dankert, Master's thesis, University of Waterloo, Ontario, Canada (2005).
- [39] M. J. Storcz, U. Hartmann, S. Kohler, and F. K. Wilhelm, Phys. Rev. B **72**, 235321 (2005).
- [40] N. Erez, G. Gordon, M. Nest, and G. Kurizki, Nature **452**, 724 (2008).
- [41] T. Jahnke and G. Mahler, Phys. Rev. E **84**, 011129 (2011).
- [42] A. E. Allahverdyan, K. V. Hovhannisyan, D. Janzing, and G. Mahler, Phys. Rev. E **84**, 041109 (2011).
- [43] I. Almog, Y. Sagi, G. Gordon, G. Bensky, G. Kurizki, and N. Davidson, J. Phys. B: At. Mol. Opt. Phys. **44**, 154006 (2011).
- [44] M. J. Biercuk, H. Uys, A. P. VanDevender, N. Shiga, W. M. Itano, and J. J. Bollinger, Nature **458**, 996 (2009).